Inorg. Chem. **2002**, *41*, 3693–3698

Contribution of Individual Zinc Ligands to Metal Binding and Peptide Folding of Zinc Finger Peptides

Akiko Nomura and Yukio Sugiura*

Institute for Chemical Research, Kyoto University, Uji, Kyoto 611-0011, Japan

Received February 21, 2002

Little is known about the contribution of individual zinc-ligating amino acid residues for coupling between zinc binding and protein folding in zinc finger domains. To understand such roles of each zinc ligand, four zinc finger mutant peptides corresponding to the second zinc finger domain of Sp1 were synthesized. In the mutant peptides, glycine was substituted for one of four zinc ligands. Their metal binding and folding properties were spectroscopically characterized and compared to those of the native zinc finger peptide. In particular, the electronic charge-transfer and d–d bands of the Co(II)-substituted peptide complexes were used to examine the metal coordination number and geometry. Fluorescence emission studies revealed that the mutant peptides are capable of binding zinc despite removing one ligand. Circular dichroism results clearly showed the induction of an α-helix by zinc binding. In addition, the structures of certain mutant zinc finger peptides were simulated by molecular dynamics calculation. The information indicates that His23 and the hydrophobic core formed between the α-helix and the β-sheet play an essential role in α-helix induction. This report demonstrates that each ligand does not contribute equally to α-helix formation and coordination geometry in the zinc finger peptide.

Introduction

Proteins containing the Cys_2His_2 zinc finger are among the most abundant proteins in eukaryotic transcription factors,[1−4] and they are involved in the direct recognition of DNA. X-ray crystallographic and nuclear magnetic resonance (NMR) studies demonstrated that the zinc finger is an independently folded domain with a compact structure and that a zinc ion is tetrahedrally coordinated by two cysteine and two histidine ligands.[5,6] The peptide backbone fold consists of a short antiparallel β-sheet in the N-terminal region and an α-helix in the C-terminal region that are arranged in a hairpin structure. Metal-binding studies on peptides corresponding to zinc finger sequences revealed a unique and fundamental property of zinc finger domains.[7−9] The circular dichroism (CD) spectrum of the metal-free peptide changes drastically upon the addition of metals, indicating that the peptide is relatively unstructured in the absence of the bound metal and that protein folding is coupled with metal binding.[9] NMR results of a single zinc finger also support that zinc binding results in protein folding.[6,10−12]

The previous studies provided limited information for the following questions: (1) How do metal−ligand interactions induce zinc finger structures? (2) What role does each ligand play in the formation and stabilization of zinc finger structures? (3) Is only the tetrahedral coordination geometry required to form zinc finger structures? By using Co(II) as a spectroscopic probe, Shi et al. demonstrated that cysteines preferentially bind to zinc prior to the metal coordination of histidines.[13] Miura et al. hypothesized that formation of the

* To whom correspondence should be addressed. E-mail: sugiura@scl.kyoto-u.ac.jp. Phone: +81-774-38-3210. Fax: +81-774-32-3038.

(1) Wolfe, S. A.; Nekludova, L.; Pabo, C. O. *Annu. Rev. Biophys. Biomol. Struct.* **2000**, *29*, 183−212.
(2) Junker, M.; Rodgers, K. K.; Coleman, J. E. *Inorg. Chem. Acta* **1998**, *275*−*276*, 481−492.
(3) Berg, J. M.; Shi, Y. *Science* **1996**, *271*, 1081−1085.
(4) Klug, A.; Schwabe, J. W. R. *FASEB J.* **1995**, *9*, 597−604.
(5) Pavletich, N. P.; Pabo, C. O. *Science* **1991**, *252*, 809−817.
(6) Lee, M. S.; Gippert, G. P.; Soman, K. V.; Case, D. A.; Wright, P. E. *Science* **1989**, *245*, 635−637.
(7) Berg, J. M.; Merkle, D. L. *J. Am. Chem. Soc.* **1989**, *111*, 3759−3761.
(8) Frankel, A. D.; Berg, J. M.; Pabo, C. O. *Proc. Natl. Acad. Sci. U.S.A.* **1987**, *84*, 4841−4845.
(9) Burke, C. J.; Sanyal, G.; Bruner, M. W.; Ryan, J. A.; Lafemina, R. L.; Robbins, H. L.; Zeft, A. S.; Middaugh, C. R.; Cordingley, M. G. *J. Biol. Chem.* **1992**, *267*, 9639−9644.
(10) Párraga, G.; Horvath, S. J.; Eisen, A.; Taylor, W. E.; Hood, L.; Young, E. T.; Klevit, R. E. *Science* **1988**, *241*, 1489−1492.
(11) Párraga, G.; Horvath, S.; Hood, L.; Young, E. T.; Klevit, R. E. *Proc. Natl. Acad. Sci. U.S.A.* **1990**, *87*, 137−141.
(12) Michael, S. F.; Kilfoil, V.; Schmidt, M. H.; Amann, B. T.; Berg, J. M. *Proc. Natl. Acad. Sci. U.S.A.* **1992**, *89*, 4796−4800.
(13) Shi, Y.; Beger, R. D.; Berg, J. M. *Biophys. J.* **1993**, *64*, 749−753.

10.1021/ic025557p CCC: $22.00
Published on Web 06/18/2002

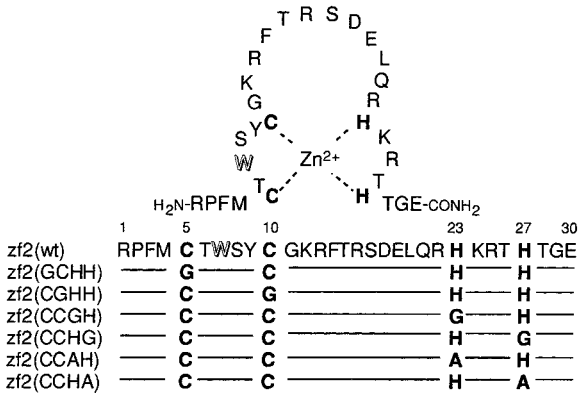

Figure 1. Amino acid sequences of zinc finger peptides. Ligands of Zn(II) and fluorophore are presented in bold and shadowed letters, respectively.

N-terminal antiparallel β-sheet induced by the metal−cysteine interaction is essential for the zinc finger structure.[14] However, it is not well understood how these metal−ligand interactions induce and stabilize zinc finger structures.

To investigate the contribution of individual ligands to protein folding in zinc finger domains, we performed metal binding studies on zinc finger peptides in which glycine or alanine was substituted for one of four zinc ligands (Figure 1). We selected the second zinc finger from human transcription factor Sp1 because of the following advantages: (1) Sp1 zinc finger domains have been well characterized by our group[15−18] and others.[19−21] (2) The three-dimensional solution structures of the second and third domains of the Sp1 zinc finger were determined by NMR spectorscopy.[21] (3) The first and second domains of the Sp1 zinc finger have a single tryptophan, whose fluorescence might be used as a probe for the folding. Here, we report the metal binding and folding properties of zinc finger peptide mutants characterized by a series of spectroscopic techniques.

Experimental Section

Materials. All *N*-fluorenylmethoxycarbonyl (Fmoc)-protected amino acids were purchased from Novabiochem or Peptide Institute, Inc. *N*-Hydroxybenzotriazole (HOBt) was obtained from the Peptide Institute, Inc., and benzotriazole-1-yl-oxytris(pyrrolidino)phosphonium hexafluorophosphate (PyBOP) was from Novabiochem. $ZnCl_2$ (99.999%), $CoCl_2$ (99.999%), and $ZnSO_4$ (0.05 M volumetric standard solution) were purchased from Aldrich. Milli-Q water was obtained from a Synthesis-A10 water purification system from Millipore. All other chemicals were of the highest commercial grade and were used without further purification.

Peptide Synthesis and Characterization. All peptides shown in Figure 1 were synthesized on a Shimadzu PSSM-8 peptide synthesizer using the Fmoc solid-phase method. TGS-RAM resin (Shimadzu) was used to afford C-terminal primary amides. Coupling was performed according to a PyBOP/HOBt/*N*-methylmorpholine strategy. After synthesis, peptides were cleaved from the resin and deprotected by treatment with trifluoroacetic acid (TFA)/1,2-ethanedithiol (95/5 v/v) at room temperature for 2 h. The solution containing free peptide was filtered, concentrated in vacuo, and precipitated with ether at 0 °C. The supernatant was decanted, and then, the solid was washed with ether. The resultant solid was resuspended in acetic acid/H_2O (50/50, v/v) and lyophilized to yield a crude peptide. Purification of the peptides was accomplished by reversed phase high-performance liquid chromatography (HPLC) on Cosmosil 5C_{18}-AR-300 (10 mm × 250 mm, Nacalai Tesque) with a 30-min linear gradient of 15−45% acetonitrile/H_2O/0.1% TFA at a flow rate of 2 mL/min. The desired peptide fraction was lyophilized and characterized by electrospray ionization mass spectrometry (ESI-MS): zf2(wt), calcd. 3714.24, obsd. (M^+) 3713.87; zf2(GCHH), calcd. 3668.14, obsd. (M^+) 3667.96; zf2(CGHH), calcd. 3668.14, obsd. (M^+) 3668.01; zf2(CCGH), calcd. 3634.15, obsd. (M^+) 3633.43; zf2(CCHG), calcd. 3634.15, obsd. (M^+) 3633.48; zf2(CCAH), calcd. 3648.18, obsd. (M^+) 3648.09; zf2(CCHA), calcd. 3648.18, obsd. (M^+) 3647.82.

Prior to use, peptides were reduced by treatment with 30 equiv of dithiothreitol for 30 min at 90 °C and purified using reverse-phase HPLC. Peptide concentrations were determined by quantifying the free thiols with 5,5′-dithiobis(2-nitrobenzoic acid)[22] and the optical intensities at 280 nm (zf2(wt) and its mutant peptides; ϵ_{280} = 7190 M^{-1} cm^{-1}).[23] All peptides were handled in an anaerobic glovebox and stored at −80 °C.

Buffer and Metal Stock Solutions. All buffer and metal stock solutions were prepared using the highest grade reagents and argon-purged Milli-Q water. Subsequently, the buffer was treated with Chelex 100 (Bio-Rad Laboratories) to remove any trace metal contamination. Prior to every measurement, buffer and metal stock solutions were purged with argon.

Fluorescence Measurement. Fluorescence emission spectra were conducted on a Hitachi F-3010 fluorescence spectrophotometer at 20 °C in 10 mM Tris-HCl buffer (pH 7.5) containing 50 mM NaCl and 5% glycerol in a capped 1-cm path length quartz cell. Emission spectra were excited at 285 nm and scanned from 300 to 450 nm. Each scan was baseline-corrected and volume-corrected prior to tabulating the data.

CD Spectroscopy. CD spectra were obtained using a Jasco J-720. Measurements were carried out in 10 mM Tris-HCl buffer (pH 7.5) containing 50 mM NaCl and 5% glycerol in a capped 1-mm path length cell at 20 °C under nitrogen. All spectra represent the average of 8−16 scans. Spectra were baseline-corrected and noise-reduced using the Jasco software. CD intensities are expressed as mean residue ellipticities (dmol·cm^2·mol^{-1}) calculated by $[\theta] = \theta/lcn$, where θ is the ellipticity observed (mdeg), l is the path length of the cell (cm), c is the peptide concentration (M), and n is the number of peptide bonds in the sequence.

Ultraviolet−Visible (UV−vis) Absorption Spectroscopy. UV−vis absorption spectra were recorded on a Beckman Coulter DU7400 diode array spectrophotometer at 20 °C in 10 mM Tris-HCl buffer (pH 7.5) containing 50 mM NaCl in a capped 1-cm path length cell. Co(II)-substituted zinc finger complexes were obtained by titration with $CoCl_2$. The peptides were saturated with Co(II) in our conditions. All presented spectra were normalized by $\epsilon = A/lc$,

(14) Miura, T.; Satoh, T.; Takeuchi, H. *Biochim. Biophys. Acta* **1998**, *1384*, 171−179.
(15) Nagaoka, M.; Sugiura, Y. *Biochemistry* **1996**, *35*, 8761−8768.
(16) Kuwahara, J.; Yonezawa, A.; Futamura, M.; Sugiura, Y. *Biochemistry* **1993**, *32*, 5994−6001.
(17) Nagaoka, M.; Kuwahara, J.; Sugiura, Y. *Biochem. Biophys. Res. Commun.* **1993**, *194*, 1515−1520.
(18) Yokono, M.; Saegusa, N.; Matsushita, K.; Sugiura, Y. *Biochemistry* **1998**, *37*, 6824−6832.
(19) Berg, J. M. *Proc. Natl. Acad. Sci. U.S.A.* **1992**, *89*, 11109−11110.
(20) Suske, G. *Gene* **1999**, *238*, 291−300.
(21) Narayan, V. A.; Kriwacki, R. W.; Caradonna, J. P. *J. Biol. Chem.* **1997**, *272*, 7801−7809.
(22) Riddles, P. W.; Blakeley, R. L.; Zerner, B. *Methods Enzymol.* **1983**, *91*, 49−60.
(23) Yin, H. L.; Lida, K.; Janmay, P. A. *J. Cell Biol.* **1988**, *106*, 805−812.

where ϵ is the extinction coefficient (M^{-1} cm^{-1}), l is the path length of the cell (cm), and c is the peptide concentration (M).

Computational Simulation. Discover software package from Accelrys, Inc. was used in order to simulate the structure of Zn(II)-mutant complexes, zf2(CCGH) and zf2(CCHG). These peptides were obtained by replacement of the His23 or His27 with Gly in the second zinc finger of Sp1[21] (PDB Id 1SP2) from the Protein Data Bank[24] and modeled using standard parameters for amino acids supplied with the Insight II software package (Accelrys, Inc.). The resulting structures were simulated with annealing protocol at 900 K and then energy-minimized at 298 K using an extensible systematic force field. The zinc potential in the complexes was assigned to a pentacoordination based on UV−vis absorption studies on Co(II) complexes.

Results and Discussion

Binding Ability to Zn(II). The second zinc finger of Sp1, zf2(wt), contains one Trp which is located near the Zn(II) in its folded form.[21] The fluorescent residue Trp can be useful as a reporter of structural changes coupled with Zn(II) binding, because the fluorescence emission spectrum strongly reflects the hydrophobicity of the environment around the Trp residue.[25,26] We observed that the fluorescence intensity of zf2(wt) increased by 2.2-fold in the presence of zinc ion.

Figure 2a shows the fluorescence spectral changes of zf2(wt) upon addition of zinc ion. The fluorescence increases with a blue shift until 1 equiv of Zn(II) is added. The observation clearly reveals that the Trp is useful for studying zinc binding of the zinc finger peptide. Therefore, we performed fluorescence studies on the mutant peptides. As shown in Figure 2b, the fluorescence intensity of the mutants reached a plateau at the point of 1 equiv of Zn(II), although the maximum intensities were dependent on the mutants (Table 1). Presumably, the fluorescence intensity of the zinc complexes reflects the flexibility of the folded structure, because the lack of a coordination ligand probably affords a relatively flexible coordination structure in the Zn(II) center of the mutants. The ESI-MS spectra of all Zn(II)−peptide complexes also demonstrated the desired molecular weight for the 1:1 complex (data not shown). No other peaks corresponding to dimer or oligomer peptides were observed. These results strongly support that each of the mutants retains the ability to bind one zinc ion despite lacking one of four zinc ligands.

Induction of α-Helix by Zn(II) Binding. The α-helix formation of peptides coupled with Zn(II) coordination was investigated by monitoring the CD spectra. The CD spectrum of zf2(wt) changed drastically upon the addition of Zn(II) (Figure 3a). The presence of Zn(II) induced two negative Cotton peaks around 208 and 222 nm, characteristic of the α-helix structure. It is considered that the coordination of Zn(II) to the two His residues plays an important role in stabilizing the α-helix structure, because these His residues

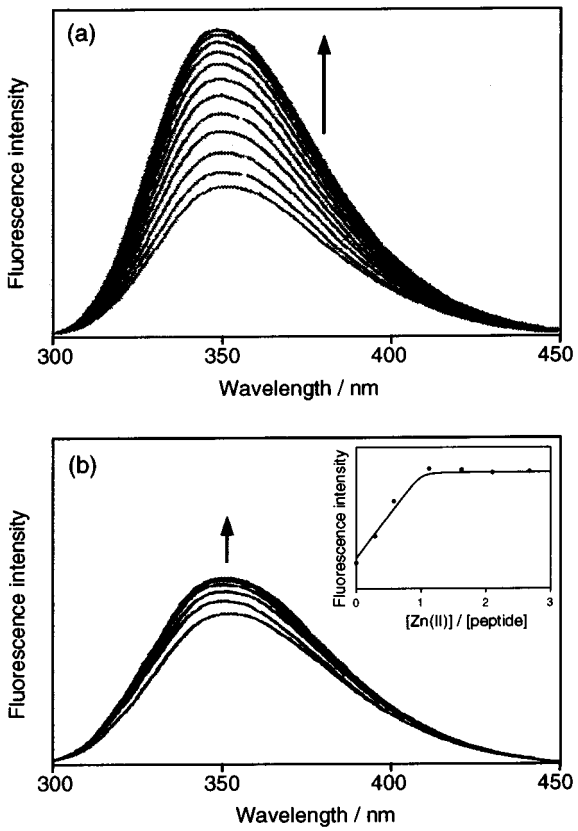

Figure 2. Fluorescence emission spectra of zinc finger peptides: (a) zf2(wt), (b) zf2(CCGH) upon addition of $ZnSO_4$. Peptide concentration was 7 μM in 10 mM Tris-HCl (pH 7.5) containing 50 mM NaCl and 5% glycerol at 20 °C. All spectra were excited at 285 nm and recorded from 300 to 450 nm. Inset: Binding curve of 25 μM zf2(CCGH) upon addition of $ZnSO_4$ up to 65 μM.

Table 1. Fluorescence Emission Properties of Zn(II)−Peptide Complexes[a]

peptide	$\lambda_{max\cdot apo}$[b] (nm)	$\lambda_{max\cdot Zn}$[c] (nm)	I_{Zn}/I_{apo}[d]
zf2(wt)	353.4	351.0	2.15
zf2(GCHH)	352.6	351.2	1.10
zf2(CGHH)	352.0	350.0	1.61
zf2(CCGH)	354.0	351.2	1.34
zf2(CCHG)	352.6	352.0	1.31
zf2(CCAH)	353.2	351.6	1.34
zf2(CCHA)	353.0	351.6	1.20

[a] Data were acquired with excitation at 285 nm in 10 mM Tris buffer (pH 7.5) containing 50 mM NaCl and 5% glycerol at 20 °C. [b]Wavelength of maximum emission for the peptide in the absence of zinc(II) ion. [c]Wavelength of maximum emission for the Zn(II)−peptide complex. [d]Fluorescence enhancement at the wavelength $\lambda_{max\cdot apo}$. I is the fluorescence intensity at $\lambda_{max\cdot apo}$ or $\lambda_{max\cdot Zn}$.

are located in the α-helix region. As expected, the cysteine-substituted peptides, zf2(GCHH) and zf2(CGHH), induce Cotton peaks characteristic of the α-helix structure in the presence of zinc (Figure 3b). The result ensures the importance of the two His residues for α-helix induction; however, the ellipticities observed for both of the cysteine mutants are more negative than those observed for zf2(wt). This implies that deletion of one cysteine ligand may increase the conformational degrees of freedom to construct a longer α-helix structure. The reason for stronger Cotton peaks for the cysteine mutants is still unclear, and an investigation is now underway.

(24) Bernstein, F. C.; Koetzie, T. F.; Willams, G. J.; Meyer, E. E., Jr.; Brice, M. D.; Rodgers, J. R.; Kennard, O.; Shimanouchi, T.; Tasumi, M. *J. Mol. Biol.* **1977**, *112*, 535−542.
(25) Ross, J. B. A.; Szabo, A. G.; Hogue, C. W. V. *Methods Enzymol.* **1997**, *278*, 151−190.
(26) Hitomi, Y.; Outten, C. E.; O'Halloran, T. V. *J. Am. Chem. Soc.* **2001**, *123*, 8614−8615.

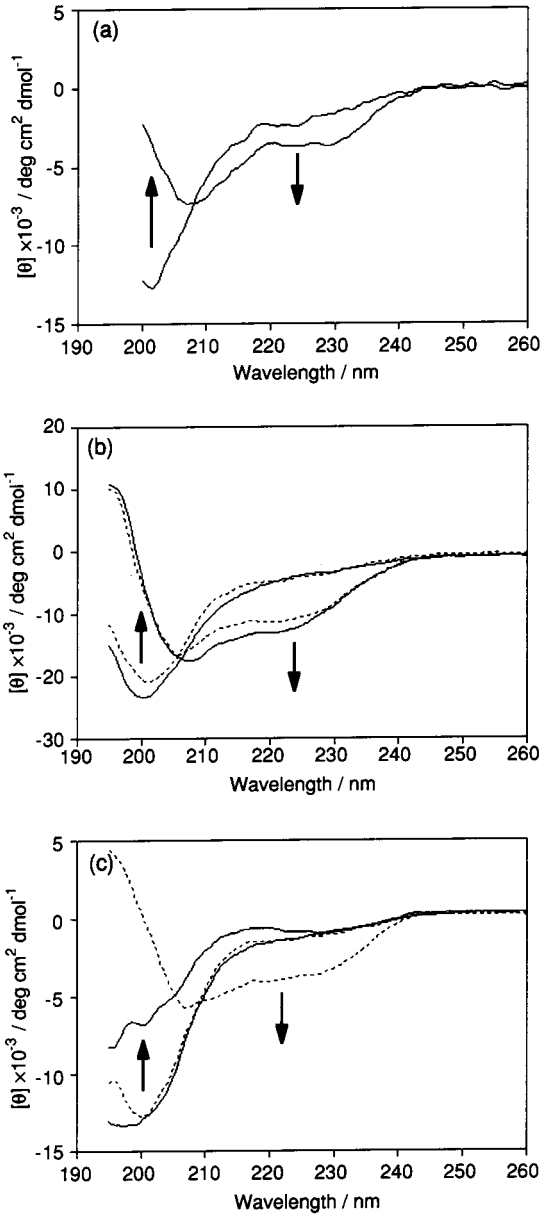

Figure 3. CD spectra of zinc finger peptides: (a) zf2(wt), (b) zf2(GCHH) (—), zf2(CGHH) (- - -), (c) zf2(CCGH) (—), zf2(CCHG) (- - -) in 10 mM Tris-HCl (pH 7.5) containing 50 mM NaCl and 5% glycerol in both the absence and presence of 1.5 equiv of $ZnCl_2$ at 20 °C. All peptides were 25 μM.

The peptide lacking one of two His residues, zf2(CCGH), showed no Cotton peaks indicative of the α-helix in the presence of Zn(II). However, the intensity of its CD spectrum showed small changes (Figure 3c). The result indicates that certain conformational changes were induced on zf2(CCGH) by binding to Zn(II). Interestingly, on the other hand, the CD spectral changes of zf2(CCHG) were remarkably similar to those observed for zf2(wt). This observation reveals that zf2(CCHG) is capable of forming an α-helix in the presence of zinc ion despite lacking one important His residue. Imperiali et al. succeeded in constructing a family of peptides that are capable of forming the $\beta\beta\alpha$ structure in the absence of metal ions.[27−30] The structure is stabilized only by a hydrophobic core formed between the α-helix and the β-sheet, suggesting that the hydrophobic core formation

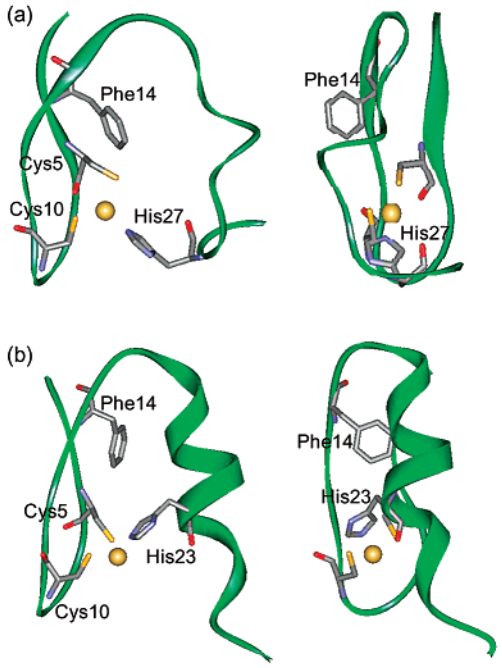

Figure 4. Proposed structures of the Zn(II)-mutant complexes (left, the side view; right, the view rotated 90° from the left): (a) zf2(CCGH) and (b) zf2(CCHG). The yellow ball indicates zinc ion. Side chains of the coordinating amino acids are represented by sticks: gray, blue, yellow, and red show carbon, nitrogen, sulfur, and oxygen, respectively.

probably plays a role in the stabilization of the α-helix in zf2(CCHG). The NMR structure of zf2(wt) clarifies that His23 is involved in hydrophobic interactions.[21] These facts lead us to the conclusion that His23 plays a significant role in α-helix induction by constructing a hydrophobic core.

Molecular Simulation. Structures of the mutant peptides, zf2(CCGH) and zf2(CCHG), were simulated by molecular dynamics calculation. The local minimum structures obtained showed good agreement with the results obtained from the CD experiment (Figure 4). The structure of zf2(CCHG) showed a structure very similar to that demonstrated by NMR studies of zf2(wt).[21] A weakly polar interaction between the conserved phenylalanine and the proximal histidine in "edge-to-face" fashion is often observed in the classical zinc finger.[31,32] The same interaction between Phe14 and His23 was observed in the calculated structure of zf2(CCHG). On the other hand, the simulated structure of zf2(CCGH) did not form an α-helix but only a coiled conformation. Also, Phe14 was placed outside the folded structure (Figure 4a, right). These results support our previously mentioned observation that the hydrophobic core involving His23 plays an important role in inducing α-helix conformation in the presence of zinc ion.

(27) Mezo, A. R.; Cheng, R. P.; Imperiali, B. *J. Am. Chem. Soc.* **2001**, *123*, 3885−3891.
(28) Struthers, M. D.; Ottesen, J. J.; Imperiali, B. *Folding Des.* **1998**, *3*, 95−103.
(29) Struthers, M. D.; Cheng, R. P.; Imperiali, B. *J. Am. Chem. Soc.* **1996**, *118*, 3073−3081.
(30) Struthers, M. D.; Cheng, R. P.; Imperiali, B. *Science* **1996**, *271*, 342−345.
(31) Jasanoff, A.; Kochoyan, M.; Freankel, E.; Lee, J. P.; Weiss, M. A. *J. Mol. Biol.* **1992**, *225*, 1035−1047.
(32) Jasanoff, A.; Weiss, M. A. *Biochemistry* **1993**, *32*, 1423−1432.

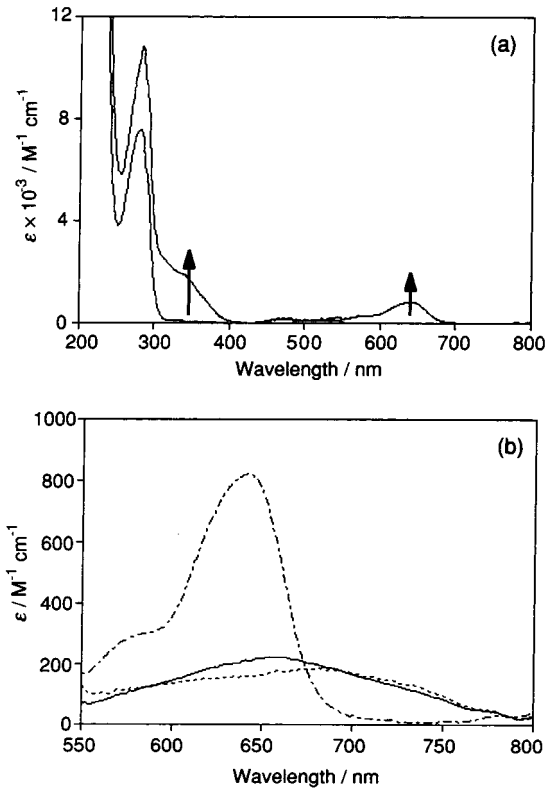

Figure 5. (a) UV−vis absorption spectra of 105 μM zf2(wt) upon addition of 2 equiv of $CoCl_2$ in 10 mM Tris-HCl (pH 7.5) containing 50 mM NaCl at 20 °C. (b) d−d absorption region of 105 μM zf2(wt) (−•−•−), 114 μM zf2(CCGH) (•••), 114 μM zf2(CCHG) (—) upon addition of 300 μM $CoCl_2$. Other conditions followed those in (a).

Coordination Geometry. To examine whether the histidine mutants retain a tetrahedral metal coordination geometry, ligand−metal coordination structures were investigated by UV−vis absorption spectroscopy. Zn(II) is a spectroscopically silent ion with an electronic configuration of d^{10}; therefore, the determination of the metal coordination of zinc fingers has often been studied using Co(II) as a spectroscopic probe for the zinc site.[7,8,13,33]

Figure 5a shows UV−vis absorption spectra of a Co(II) complex of zf2(wt). The intense absorption bands in the near-ultraviolet around 316 and 340 nm are indicative of the $S^- \rightarrow$ Co(II) ligand-to-metal charge-transfer (LMCT) transition.[34,35] The magnitude of the extinction coefficient (ϵ) at 320 nm reflects the number of thiolate groups coordinated to the metal and averages about 900−1200 M^{-1} cm^{-1} per S^-−Co(II) bond.[36,37] Table 2 summarizes the ϵ at 320 nm of the mutants. For zf2(wt), the intensity of the LMCT band indicates metal coordination by both of the two thiolate ligands. The mutants, zf2(CCGH) and zf2(CCHG), also showed the same LMCT band as that observed for zf2(wt) (data not shown), and hence, their intensities agree with the two thiolate ligands to Co(II).

Table 2. Extinction Coefficient (ϵ) of Co(II)−Peptide Complexes[a]

peptide	LMCT band ϵ ($M^{-1}cm^{-1}$)[b]	d−d band λ (nm)/ϵ ($M^{-1}cm^{-1}$)[c]		
zf2(wt)	2275	582/298	640/820	
zf2(CCGH)	2360	625/135	680/160	
zf2(CCHG)	2260	655/191		
zf2(CCAH)	2350	620/165	675/182	730 /130
zf2(CCHA)	2330	580/310	645/420	

[a] Data were acquired in 10 mM Tris buffer (pH 7.5) containing 50 mM NaCl at 20 °C. [b] ϵ at 320 nm. [c] Wavelength of peak(s) for d−d transition and ϵ at the wavelength.

On the basis of the ligand-field theory, it is known that optical transitions of a tetrahedral Co(II) species exhibit intense d−d absorption band ($\epsilon > 300$ M^{-1} cm^{-1}) in the region 625 ± 50 nm coming from a relatively small ligand-field stabilization energy.[38] Co(II) complexes with octahedral symmetry reveal only weak absorption ($\epsilon \leq 30$ $M^{-1}cm^{-1}$) around 525 ± 50 nm. On the other hand, pentacoordinate Co(II) complexes present an intermediate absorption characteristic ($50 \leq \epsilon \leq 250$ M^{-1} cm^{-1}) of that between tetrahedral and octahedral Co(II) complexes. In the case of zf2(wt), diagnostic d−d transition bands were observed at 640 and around 580 nm, and their ϵ values were 820 and 300 M^{-1} cm^{-1}, respectively (Table 2). This feature indicates the typical tetrahedral S_2N_2 coordination geometry in the zinc finger.[38] Both of the histidine mutants, zf2(CCGH) and zf2(CCHG), showed remarkably different spectra from zf2(wt). The broad and weak d−d absorption profiles are suggestive of pentacoordination (Figure 5b). The absorption spectra of Co(II)-substituted peptides in HEPES buffer were identical to those in Tris buffer. HEPES is unlikely to coordinate zinc ion. The result indicates that Tris does not coordinate zinc ion. In addition, the previous fluorescence study showed that (1) the fluorescence increase reaches a plateau at the point of 1 equiv of Zn(II) and (2) the Trp is located in the hydrophobic environment in the compact structure induced by the coordination of Cys and His to Zn(II). Therefore, two water, two thiolate, and one imidazole molecules are coordinated to Co(II). Merkle et al. reported on a histidine-truncated consensus zinc finger peptide in which the last four amino acids, including the last histidine residue, were deleted.[39] In contrast to our results, the Cys_2His zinc finger peptide exhibits the d−d band characteristic of tetrahedral coordination in Co(II) form. The consensus zinc finger peptide can bind zinc ion more tightly than zf2(wt) through the optimized hydrophobic interaction.[40] The tight hydrophobic interaction may keep tetrahedral metal coordination geometry despite lacking the second His residue.

In an aim to increase the hydrophobicity, two alanine mutants, zf2(CCAH) and zf2(CCHA), were synthesized and characterized by CD and UV−vis spectroscopies. As shown in Figure 6, they exhibited CD spectral changes quite similar to those observed for the corresponding glycine mutants, suggesting that increasing the methyl group in the alanine

(33) Maret, W.; Vallee, B. L *Methods Enzymol.* **1993**, *226*, 52−71.
(34) Giedroc, D. P.; Keating, K. M.; Williams, K. R.; Konigsberg, W. H.; Coleman, J. E. *Proc. Natl. Acad. Sci. U.S.A.* **1986**, *83*, 8452−8456.
(35) Chen, X.; Chu, M.; Giedroc, D. P. *J. Biol. Inorg. Chem.* **2000**, *5*, 93−101.
(36) Vasak, M.; Kägi, H. H. R.; Holmquist, B.; Vallee, B. L. *Biochemistry* **1981**, *20*, 6659−6664.
(37) May, S. W.; Kuo, J. Y. *Biochemistry* **1978**, *17*, 3333−3338.
(38) Bertini, I.; Luchinat, C. *Adv. Inorg. Biochem.* **1984**, *6*, 71−111.
(39) Merkle, D. L.; Schmidt, M. H.; Berg, J. M. *J. Am. Chem. Soc.* **1991**, *113*, 5450−5451.
(40) Krizek, B. A.; Amann, B. T.; Kilfoil, V. J.; Merkle, D. L.; Berg, J. M. *J. Am. Chem. Soc.* **1991**, *113*, 4518−4523.

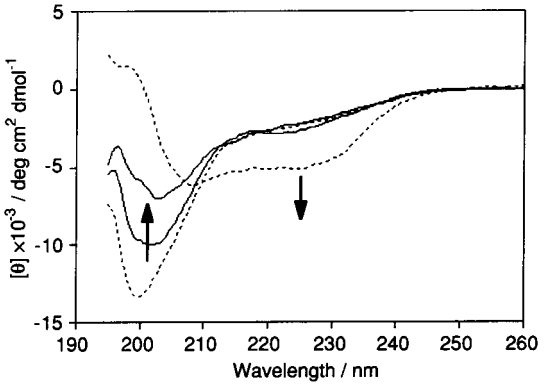

Figure 6. CD spectra of alanine mutants: zf2(CCAH) (—) and zf2(CCHA) (- - -) upon 1.5 equiv of $ZnCl_2$. All other conditions followed those in Figure 3.

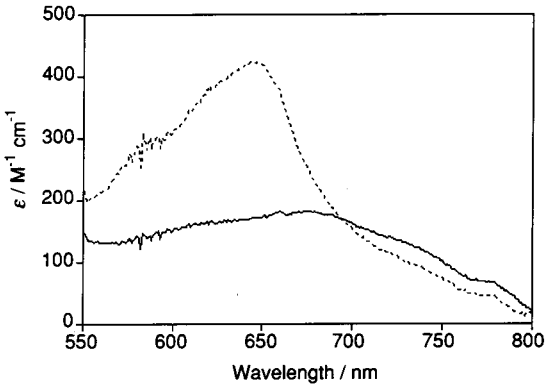

Figure 7. Normalized UV−vis absorption spectra of 85.2 μM zf2(CCAH) (—) and 82.2 μM zf2(CCHA) (···) in the presence of 3 equiv of $CoCl_2$. All other conditions followed those in Figure 5.

mutants has little effect on the increase in helicity. Co(II) complexes of zf2(CCAH) and zf2(CCHA) showed an LMCT band with magnitudes of $\epsilon = 2350$ and 2330 M^{-1} cm^{-1} at 320 nm, respectively, supporting the coordination of the two thiolate ligands observed in zf2(wt) as well as the glycine mutants. On the other hand, the d−d bands presented different results from those obtained from the glycine mutant counterparts (Figure 7). While zf2(CCAH) showed a d−d absorption band characteristic of a pentacoordination geometry like that of zf2(CCGH), zf2(CCHA) presented two strong d−d absorption bands at 645 nm ($\epsilon = 420$ M^{-1} cm^{-1}) and around 580 nm ($\epsilon = 310$ M^{-1} cm^{-1}). The latter result suggests an S_2NO tetrahedral coordination in zf2(CCHA),[39] namely Co(II) ligated by two thiolate, one imidazole, and one water molecules. The difference between zf2(CCHG) and zf2(CCHA) is only a methyl group. This result shows that the small volume change near the coordination cavity can control the number of water molecules ligated to the metal. However, the possibility that observed changes of coordination geometry may occur only for the cobalt-substituted peptides cannot be ruled out, because cobalt has greater tendency to bind as pentacoordinate than zinc.[7]

This report demonstrates that even zinc finger peptide mutants having only three metal coordinating residues can form a compact structure with an α-helix conformation in the presence of zinc when the two His residues in the α-helix region or the interaction between His23 and the hydrophobic core is conserved. It was reported that a GCHH-type zinc finger motif is encoded by the human homologue of the *Mok2*.[41] Although it was mentioned that the zinc finger is degenerated, our experiment supports that the zinc finger can bind zinc and fold in a structure similar to that of the C_2H_2 zinc finger. Moreover, this study would shed new light on the possibility that small metallopeptides with the desired coordination geometry can be synthesized by choosing an appropriate amino acid sequence.

Acknowledgment. For supplying computation time, we thank the Supercomputer Laboratory, Institute for Chemical Research, Kyoto University. This study was supported in part by Grants-in-Aid for the COE Project Element Science, Priority Project Biometals, and Scientific Research from the Ministry of Education, Culture, Sports, Science, and Technology, Japan. We thank M. Nagaoka for helpful discussions.

IC025557P

(41) Ernoult-Lange, M.; Arranz, V.; Le Coniat, M.; Berger, R.; Kress, M. *J. Mol. Evol.* **1995**, *41*, 784−794.